
ReSpace: Text-Driven 3D Scene Synthesis and Editing with Preference Alignment

Martin JJ. Bucher
Stanford University
mnbucher@stanford.edu

Iro Armeni
Stanford University
iarmeni@stanford.edu

respace.mnbucher.com

Abstract

Scene synthesis and editing has emerged as a promising direction in computer graphics. Current trained approaches for 3D indoor scenes either oversimplify object semantics through one-hot class encodings (e.g., 'chair' or 'table'), require masked diffusion for editing, ignore room boundaries, or rely on floor plan renderings that fail to capture complex layouts. In contrast, LLM-based methods enable richer semantics via natural language (e.g., 'modern studio with light wood furniture') but do not support editing, remain limited to rectangular layouts or rely on weak spatial reasoning from implicit world models. We introduce RESPACE, a generative framework for text-driven 3D indoor scene synthesis and editing using autoregressive language models. Our approach features a compact structured scene representation with explicit room boundaries that frames scene editing as a next-token prediction task. We leverage a dual-stage training approach combining supervised fine-tuning and preference alignment, enabling a specially trained language model for object addition that accounts for user instructions, spatial geometry, object semantics, and scene-level composition. For scene editing, we employ a zero-shot LLM to handle object removal and prompts for addition. We further introduce a novel voxelization-based evaluation that captures fine-grained geometry beyond 3D bounding boxes. Experimental results surpass state-of-the-art on object addition while maintaining competitive results on full scene synthesis.

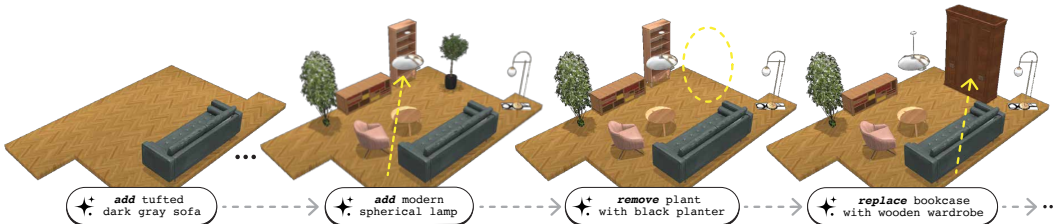


Figure 1: We introduce a novel text-driven framework for 3D indoor scene synthesis, completion, and editing—supporting object addition, removal, and swapping via natural language prompts.

1 Introduction

Scene synthesis for 3D environments has been a long standing challenge in computer graphics for many decades. Indoor scenes have been of particular interest due to the wide range of applications in virtual and mixed reality, robotics, entertainment, interior design, and more. As the manual creation and editing of such scenes requires substantial human effort and expertise, significant effort has been put on automating this process. With early approaches revolving around heuristics-based methods and procedural modeling [30, 45, 46, 52, 29, 11], recent effort has shifted towards deep generative models, i.e., learning the distribution of indoor scenes directly from data. For instance, autoregressive models [27, 40, 33] learn to stochastically predict a sequence of objects for full scene generation or completion. Another line of work explores diffusion-based models for scene synthesis [38, 17, 24]

by learning how to gradually denoise object properties from random noise. Methods based on scene graphs have also been proposed, either by assuming a high-level scene graph as input or by generating a scene graph in a first stage and then obtaining object properties via diffusion [54, 21]. With the recent advent of instruction-tuned Large Language Models (LLMs), agent-based approaches have been pursued, relying primarily on the inherent world model of LLMs [37, 6, 49, 10]. However, existing methods face several limitations: they simplify object semantics via one-hot class labels, ignore room boundaries or rely on fixed-resolution floor plans regardless of scene complexity, depend on zero-shot LLMs or external optimization algorithms given nascent Spatial Foundation Models, and lack direct natural language modification capabilities. Consequently, controllable scene synthesis and editing with rich semantic and geometric understanding remains a significant challenge.

We propose RESPACE, a framework leveraging natural language for intuitive scene synthesis and editing through text commands for object addition and removal. At its core is our Structured Scene Representation (SSR)—a JSON-based format encoding room boundaries, object semantics, and precise placement in a lightweight (\sim KBs), editable form. Framing scene manipulation as a next-token prediction task, we train a specialized model, SG-LLM, for object addition that takes a short object prompt as input and performs single object placement as output. We employ a zero-shot LLM to decompose user instructions into addition/removal commands, handle removals directly through SSR text editing, and generate object lists for addition that SG-LLM processes autoregressively for full scene synthesis. We decouple 3D asset selection from the SSR using a stochastic sampler that matches both size and semantics from an existing asset catalog. Example prompt-output pairs are shown in Figure 2 alongside a summary. For evaluation, we introduce a voxelization-based metric capturing fine-grained geometric interactions beyond bounding boxes, quantifying more realistic placements such as chairs partially under tables (Figure 4 (C)). After Supervised Fine-Tuning (SFT) on instructions, we use this metric—alongside other constraints—as verifiable reward for Group Relative Policy Optimization (GRPO) on SG-LLM. Experiments on the 3D-FRONT [12] dataset demonstrate a new state-of-the-art for single object placement and competitive performance for full scene synthesis. Code and dataset are available under: <https://github.com/gradientspaces/respace>. In summary, our contributions are as follows:

- We present RESPACE, a novel method for controllable scene synthesis and editing, designing object addition and removal via next-token prediction and text-driven commands.
- We feature a dual-stage pipeline (SFT+GRPO) for object addition and are first to apply preference optimization with Reinforcement Learning with Verifiable Rewards (RLVR) on it, surpassing state-of-the-art while achieving competitive results for full scene synthesis.
- We introduce a lightweight and interpretable Structured Scene Representation (SSR) with natural-language object descriptions and explicit numerical values for scene boundaries and object positioning (e.g., size and location), enabling direct editing and manipulation.
- We propose the Voxelization-Based Loss (VBL), a novel evaluation metric capturing fine-grained geometric interactions beyond 3D bounding boxes (e.g., between chair and table).

2 Related Work

3D Indoor Scene Synthesis. Early scene synthesis approaches relied on heuristics and procedural modeling [30, 45, 46, 52, 29, 11]. With deep learning’s emergence, transformers [33, 41, 27] and diffusion models [38, 17, 44, 24] gained prominence. Deep Priors [40] introduced CNN-based attribute prediction, while Fast&Flexible [33] developed a chained CNN pipeline conditionable on floor plan images. SceneFormer [41] proposed autoregressive transformers conditioned on floor plans and text descriptions, while ATISS [27] pioneered treating scenes as unordered object sets. Recent advances include diffusion-based approaches like DiffuScene [38], Mi-Diff [17] (supporting floor plan conditioning via PointNet features), and LEGO-Net [44] (via rearrangement). Human-centric approaches include MIME [51] and SUMMON [50], while scene graph methods [9, 21, 53, 54, 23] like InstructScene [21] and EchoScene [54] use intermediate graph representations. Despite these advances, existing methods lack support for text-driven editing or explicit 3D boundaries, limiting their ability to handle complex layouts and intuitive manipulation through user-level instructions.

Language-based Scene Synthesis. Early work like CLIP-Layout [22] explored text-prompted synthesis using CLIP [31] embeddings. With the rise of instruction-tuned LLMs, agent-based approaches have evolved: LayoutGPT [10] pioneered zero-shot object placement via CSS-based

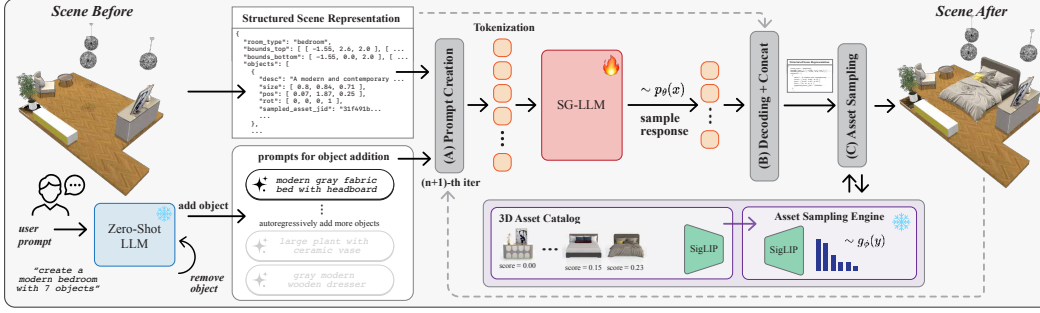


Figure 2: **ReSpace Overview.** Given a user instruction via text and an existing scene represented via SSR, we autoregressively perform 3D scene synthesis and editing. A zero-shot LLM converts user instructions to sequential commands for object removal and addition, with the latter done via specialized SG-LLM (p_θ) and removal via zero-shot SSR editing.

representation, while I-Design [6], Holodeck [49], and Open-Universe [1] employ multi-agent LLM systems to construct scene graphs or Domain Specific Language (DSL) instances before passing them to separate layout optimizers. LayoutVLM [37] generates text-based layouts with constraints before optimization, while LLPlace [48] retrieves assets via text prompts before using a fine-tuned LLM for placement. Unlike these methods requiring separate optimization stages, our approach uses a specialized LLM that directly predicts object semantics and positioning in a single forward pass. This reduces the need for separate convex optimization loops while remaining fully generative and extending beyond rectangular floor plans to non-convex geometries.

Preference Alignment and Test-Time Compute Scaling. LLM development has evolved from pre-training only (GPT-3 [5] era) to dual-stage pipelines with instruction-tuning and preference alignment. Nominal works include InstructGPT [26], FLAN [43], Reinforcement Learning from Human Feedback (RLHF) [7], Direct Preference Optimization (DPO) [32], and, most recently, Group Relative Policy Optimization (GRPO) [34] and RLVR [20, 36]—all aligning models to maximize (learned) rewards. Recent work also focuses on increased test-time compute [35] via self-consistency [42], Best-of-N sampling, and reward models [4]. Formulating scene synthesis via language modeling, we are the first, to our knowledge, performing preference alignment on this task via verifiable rewards.

3 RESPACE

We introduce RESPACE, a method for autoregressive indoor scene generation and editing via natural language. Specifically, for an existing (empty or partial) scene, our system adds and removes objects sequentially via object prompts, enabling scene modification and full scene synthesis (Figure 2).

Problem Statement. Let $p_{\mathcal{D}}(x)$ be the distribution of 3D indoor scenes from a dataset \mathcal{D} . Learning a generative model that gets very close to this data distribution allows us to sample from $p_\theta \approx p_{\mathcal{D}}$. Now, given a user instruction u_i in natural language, our goal is to learn the conditional distribution $\hat{S}_i \sim p_\theta(S_i|u_i)$ with input scene S_i and modified scene \hat{S}_i . Let $\mathcal{S} = \{S_1, S_2, \dots, S_N\}$ be a collection of indoor scenes, where each scene $S_i = (T, \mathcal{B}, \mathcal{O})$ is composed by its room type $T \in \mathcal{T}$, room boundaries $\mathcal{B} = \{\mathcal{B}_{\text{top}}, \mathcal{B}_{\text{bottom}}\}$, and unordered set of objects $\mathcal{O} = \{O_1, O_2, \dots, O_K\}$. Unlike previous work, our bounds are defined as ordered point sets $b_i \in \mathbb{R}^3$ forming closed rectilinear polygons— $\mathcal{B}_{\text{top}} = \{b_1, b_2, \dots, b_M\}$ for the ceiling and $\mathcal{B}_{\text{bottom}}$ for the floor. Further, each object in the scene $O_i = (d_i, h_i, t_i, r_i)$ is represented as a labeled 3D bounding box with asset description d_i , size $h_i \in \mathbb{R}^3$, position $t_i \in \mathbb{R}^3$, and orientation $r_i \in \mathbb{R}^4$. The object description d_i captures fine-grained object semantics such as material, color, and style explicitly via text. Rotations are given as quaternions. We formulate the task of 3D scene synthesis as learning a generative model such that a scene with K objects can be composed via:

$$p_\theta(T, \mathcal{B}, \mathcal{O}) = p_\theta(\mathcal{O}|T, \mathcal{B}) p_\theta(T, \mathcal{B}) = \prod_{i=0}^K p_\theta(O_i|p_i, \{O_{j<i}\}, T, \mathcal{B}) p(T, \mathcal{B}) \quad (1)$$

such that the current object depends on the previously placed objects $\{O_{j<i}\}$ and natural language prompt p_i , given room boundaries \mathcal{B} and room type T . Further, let $p(T, \mathcal{B})$ be given as a prior distribution and $O_1 \sim p_\theta(O_1|p_1, T, \mathcal{B})$ for an initially empty scene.

3.1 Structured Scene Representation

Given a scene $S_i = (T, \mathcal{B}, \mathcal{O})$, we propose a novel Structured Scene Representation (SSR) that follows a nested dictionary schema. This is inspired by hierarchical DSLs as seen in prior work on scene composition and shape programs [56, 39, 2], but follows a simpler structure for 3D indoor scenes. Let T be given as a text string with key ‘room_type’, let boundaries \mathcal{B}_{top} and $\mathcal{B}_{\text{bottom}}$ be given as a nested list of 3D coordinates with keys ‘bounds_top’ and ‘bounds_bottom’, and let the set of objects be a flat list of dictionaries under the ‘objects’ key. Each object is defined as a dictionary with ‘desc’ for its natural language description, and ‘size’, ‘pos’, and ‘rot’ for its positional attributes. A full example of our SSR is given in Appendix A.5, with a short snippet seen in Figure 2. Note that the 3D asset choice can be detached from the actual scene representation. Thus, our proposed SSR is an *abstraction layer* over the specific 3D scene instance and allows to swap assets without changing the underlying SSR. This choice, in contrast to neural scene or voxel-based representations [28, 25], is lightweight (\sim KBs), and directly interpretable and editable via natural language. Further, it is extensible by future work by, e.g., representing doors/windows as 2D planes or adding relative spatial relationships between objects for more fine-grained scene graph representations.

3.2 Scene Synthesis via Autoregressive Language Modeling

Given an SSR instance, we can tokenize a scene S_i into M text tokens t_j such that $\text{Tok}(S_i) = \mathcal{U} = \{t_1, \dots, t_M\}$. Let $\mathcal{U}_{\text{prev}}$ be the sequence of tokens for the existing scene that composes an SSR, and let \mathcal{U}_i be the token sequence for the current object. We can formulate a generative model for autoregressive scene synthesis and completion as a conditional next-token prediction task:

$$p_{\theta}(O_i | p_i, \{O_{j < i}\}, T, \mathcal{B}) = p_{\theta}(\mathcal{U}_i | p_i, \mathcal{U}_{\text{prev}}) = \prod_{j=0}^M p_{\theta}(t_j | p_i, \mathcal{U}_{\text{prev}}, t_{< j}) \quad (2)$$

thus, during inference, sampling the next object for the scene involves sampling M tokens from $p_{\theta}(x)$ until the end-of-sequence (EOS) token is chosen. Let, $p_{\theta}(x)$ be represented by an LLM and let this specially trained model for autoregressive object addition be denoted as SG-LLM (Scene Graph LLM). We show our pipeline in Figure 2 for an example scene, where the full input prompt for the latter is composed in step (A) from the existing SSR and a single object prompt. After tokenization, forward pass in the LLM, and response sampling, tokens get decoded and concatenated with the existing object list in step (B). Lastly, a 3D asset is sampled in step (C) via asset sampling engine. This process can be repeated K times to iteratively add more objects, given K object prompts.

Stochastic Asset Sampling. We can retrieve assets for added objects from a given 3D asset catalog using the descriptions and sizes of each object defined in the SSR. Prior work uses greedy selection via closest 3D bounding box match, filtered by class label [10, 27, 38, 6, 48, 17]. In contrast, we formalize asset retrieval as a probabilistic process where each 3D asset mesh m_i is drawn from a distribution parameterized by semantic and geometric constraints: $m_i \sim g_{\phi}(d_i, h_i)$, where d_i is the natural language description and h_i is the target size. The distribution g_{ϕ} computes scores as weighted combinations of semantic and geometric similarities: $\text{score}(m_j) = \lambda \cdot \text{sim}_{\text{sem}}(d_i, d_j) + (1 - \lambda) \cdot \text{sim}_{\text{geo}}(h_i, h_j)$, where sim_{sem} uses L2-normalized SigLIP [55] embeddings for text-to-asset matching and sim_{geo} measures size compatibility via Gaussian similarity: $\exp(-\|s_i - s_j\|^2 / (2\sigma^2))$. The final distribution is obtained through temperature-scaled softmax with nucleus sampling (top- p) and top- k filtering. For deterministic ‘greedy’ retrieval, we can set $m_i = \arg\max_{m_j} g_{\phi}(d_i, h_i)$.

Preference Alignment via GRPO. With object addition formulated as token-level language modeling, we can leverage preference optimization with frameworks such as Group Relative Policy Optimization (GRPO) [34]. Let for each iteration and prompt be G candidates a_i with verifiable reward r_i and the following optimization objective:

$$J(\theta) = \frac{1}{G} \sum_{i=1}^G \left(\min \left(\frac{\pi_{\theta}(a_i | s)}{\pi_{\text{old}}(a_i | s)} A_i, \text{clip} \left(\frac{\pi_{\theta}(a_i | s)}{\pi_{\text{old}}(a_i | s)}, 1 - \varepsilon, 1 + \varepsilon \right) A_i \right) - \beta D_{KL}(\pi_{\theta} || \pi_r) \right) \quad (3)$$

where each term in the sum is expanded as a per-token loss per response a_i . The advantage A_i is given as $A_i = \frac{r_i - \text{mean}(r_1, \dots, r_G)}{\text{std}(r_1, \dots, r_G)}$, β controls the KL divergence between the current policy π_{θ} and reference policy π_r , and ε is given as upper/lower-bound for clipping.

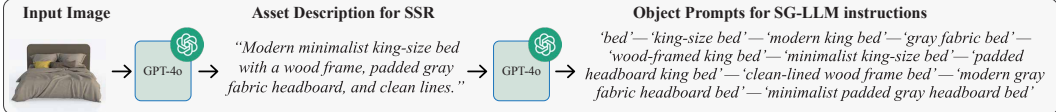


Figure 3: Example of description and prompt bank generation via asset rendering and GPT-4o [18].

Full Scene Synthesis and Object Removal via Zero-Shot Learning. Our method targets scene *editing* via autoregressive addition and removal, where removal is enabled through a zero-shot LLM (see Figure 2 for an overview). When given a removal command, this LLM directly modifies the SSR by updating the JSON to remove specified objects. For full scene generation, we leverage this same zero-shot LLM’s (LLM_{ZS}) inherent *world model* to generate an object prompt list $\mathcal{P}_i = \{p_1, \dots, p_K\} \sim LLM_{ZS}(u_i)$ from user instruction u_i . A complete scene S_i can then be created by autoregressively passing each object prompt for addition to our trained SG-LLM. System prompts for these components are reported in Appendix A.6. While using a single model for all scene synthesis and editing tasks would be theoretically preferable, this would require more complex fine-tuning in an SFT+RL pipeline to prevent mode collapse due to task/class imbalance. Thus, for this work, we focus on optimizing SG-LLM for object addition only, demonstrating the approach’s viability while simplifying the training process by complementing it with a zero-shot LLM.

3.3 Layout Violations: Voxelization-Based Loss

Representing scenes via SSR follows previous work in the sense that objects can be simplified by a collection of positioned 3D bounding boxes. We show a visualization in Figure 4 (A), with blue boxes for objects and red small red cubes for ceiling and floor room bounds. Existing work on indoor scene synthesis does not study or report layout violations extensively; it reports ‘out-of-bounds’ as the ratio of scenes that have objects partially out-of-bounds [6], or object-intersections via Intersection-over-Union [17] or average volume intersection [6] on 3D bounding boxes. However, bounding-box-based metrics are unable to accurately evaluate realistic object placement (e.g., chair and table in Figure 4 (A)) or provide an accurate signal of violations. We introduce the Voxelization-Based Loss (VBL), a novel geometry-aware evaluation metric that is defined as follows:

We voxelize the scene boundary mesh \mathcal{B} with fixed voxel size G to create uniform grid V_S , and similarly voxelize each object mesh O_j into binary occupancy grid $\mathcal{V}_j \in \{0, 1\}^{x_j \times y_j \times z_j}$. To quantify layout violations, we define two metrics: (1) Out-of-Bounds Loss (OOB) counts voxels outside scene boundaries as $OOB_j = \sum_i \mathcal{V}_j(i) - \sum_i \mathcal{V}_j(i) \cdot \mathcal{V}_S(i)$ with total $OOB = \sum_j OOB_j$, and (2) Mesh Boundary Loss (MBL) measures voxel overlap between unique object pairs (O_m, O_n) as $MBL_{(m,n)} = \sum_i \mathcal{V}_m(i) \cdot \mathcal{V}_n(i)$. Since MBL is symmetric, it is computed once per unique pair, with total $MBL = \sum_{m < n} MBL_{(m,n)}$. The total Voxel-Based Loss (VBL) is the sum of these two metrics, quantifying how many voxels ‘violate’ the layout. Figure 4 shows these violations with OOB voxels in red and MBL voxels in purple. We motivate OOB and MBL as separate sub-metrics as they are complementary—objects outside boundaries have high OOB but low MBL since they are less likely to intersect with other objects. It is thus crucial to minimize both metrics. Since MBL scales subquadratically with object count, we implement a horizontal 2D intersection check for early stopping, skipping full computation when 2D projections show zero violations. We find that a voxel size of $G = 0.05m$ provides an optimal compute/accuracy trade-off.

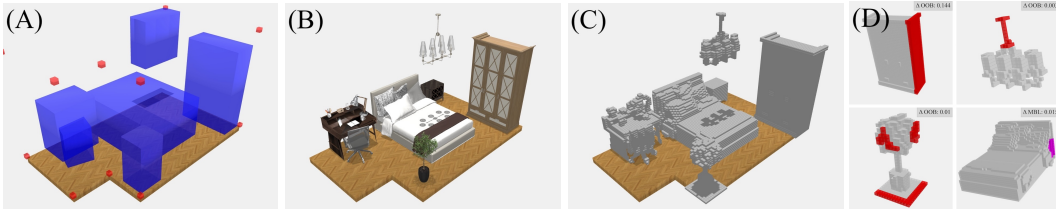


Figure 4: Scene represented with 3D bounding boxes in blue and bounds in red (A), with 3D assets (B), their voxelized counterpart (C), and some examples of OOB/MBL voxel violations (D). Note how the desk and chair interact smoothly in mesh space compared to their blue bounding boxes, while the lamp is largely OOB with its bounding box but only minor with its mesh.

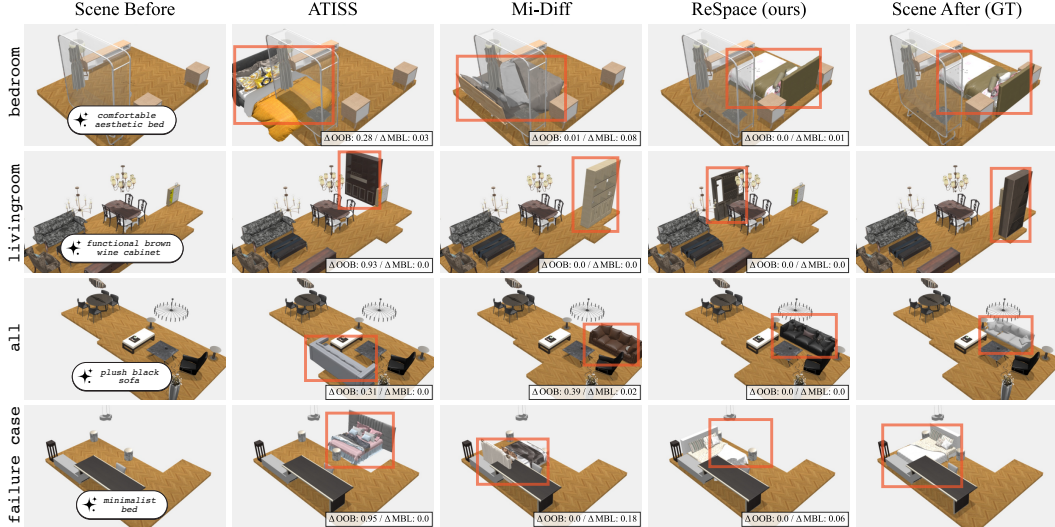


Figure 5: Qualitative results on single instructions, with our method performing the strongest. For ours, we use ReSpace/A[†]. We show a failure case on the last row where all methods perform poorly.

4 Experiments

We conduct experiments on two main tasks: (i) single object addition on partial scenes via prompt-based instructions and (ii) full scene synthesis. For ours, we also study the effectiveness of object removal and perform various ablations studies for further analysis.

Scene-Prompt Dataset. We partition 3D-FRONT [12] into ‘bed’ (bedrooms), ‘liv’ (living rooms and dining rooms), and ‘all’ splits (with 6328/500/500, 3830/500/500, and 12055/500/500 train/val/test samples respectively) after filtering out noisy samples via our voxelization-based method. Since the dataset lacks textual descriptions, we use GPT-4o [18] as a vision-language model to first generate detailed descriptions d_j for each object from provided 3D-FUTURE [13] renderings, then create 10 unique, concise prompts per object description to form our prompt bank $\mathcal{P}(o)$ (see for an example Figure 3). During training, we dynamically generate instruction triples $\mathcal{I} = (\hat{S}, p, o_{\text{add}})$ with object o_{add} to be added, and include empty rooms (10%), scenes with a final object placement missing (10%), and partial scenes with random number of existing objects (80%). We create fixed test sets with 500 instructions and corresponding object prompts using three random seeds for fair comparison with baselines. Details about preprocessing and instruction generation are found in Appendix A.1.

4.1 Experimental Settings

Implementation Details. We train SG-LLM on a two-stage pipeline with 4xA100 80GB NVIDIA GPUs by fine-tuning a pre-trained LLM on our custom instruction dataset. We conducted extensive experiments with 1B and 0.5B models, but observed best results with ‘Qwen2.5-1.5B-Instruct’ [47]. Thus, for all experiments, we use the latter, together with ‘Llama-3.1-8B-Instruct’ [14] for the zero-shot LLM. For GRPO, we set $\beta = 0.0$, canceling out the KL divergence term, give rewards of -1.0 for invalid JSON outputs, and 1.0 for candidates a_i that pass the following filter: $\text{PMS}(a_i) \geq 0.85$, $\text{DSS}(a_i) \geq 0.9$, $\text{VBL}(a_i) < 1e - 5$, and $\|(s_{a_i}^{GT} - s_{a_i})\|^2 < 0.2$, where the latter is the L2 distance between predicted size s_{a_i} and ground-truth (GT) size $s_{a_i}^{GT}$ of the 3D bounding box, and $\text{DSS}(a_i)$ denotes the cosine similarity of the SigLIP embeddings between GT ‘desc’ and predicted one. We further introduce a *high-quality-only* distillation that cancels out the loss for samples that have valid JSON but do not satisfy the above filter. This stems from our observation that (i) the SFT model produces only $\sim 25\%$ high-quality additions which leads to dominating negative rewards, leading to destruction of SFT behavior, and (ii) strong reward hacking.

Baselines. We compare our method to existing state-of-the-art 3D scene synthesis approaches: (i) ATISS [27], a transformer-based auto-regressive model that treats scenes as unordered set of objects; and (ii) MiDiffusion [17] (Mi-Diff), a mixed discrete-continuous diffusion model for scene

Table 1: Quantitative evaluation on **single-instruction object addition** on a hold-out test set of 3×500 fixed instructions and their corresponding object prompts, generated with 3 random seeds. Each method is trained on the same train splits. KID and Layout Violation (OOB, MBL, VBL) are multiplied by 10^3 for readability. Best values are in **bold**, second best in underline.

Method	Scene Renderings			Layout Violations			Prompting	
	\downarrow FID	\downarrow FID _{CLIP}	\downarrow KID $\times 1e3$	\downarrow OOB $\Delta_{\times 1e3}$	\downarrow MBL $\Delta_{\times 1e3}$	\downarrow VBL $\Delta_{\times 1e3}$	\uparrow PMS	
‘bed’	ATISS [27]	36.18 \pm .3	1.74 \pm .0	0.19 \pm .0	97.70 \pm 6.0	13.54 \pm 0.5	111.24 \pm 5.4	0.58 \pm .0
	Mi-Diff [17]	36.12 \pm .3	1.76 \pm .1	<u>0.05</u> \pm .0	64.04 \pm 5.3	14.27 \pm 1.5	78.31 \pm 4.1	0.57 \pm .0
	ReSpace/B	35.10 \pm .3	1.66 \pm .0	-0.06 \pm .1	<u>20.68</u> \pm 4.1	6.21 \pm 1.0	<u>26.89</u> \pm 4.8	<u>0.87</u> \pm .0
	ReSpace/A [†]	<u>35.51</u> \pm .2	<u>1.67</u> \pm .0	0.06 \pm .1	8.38 \pm 1.5	<u>8.13</u> \pm 1.2	16.51 \pm 3.0	0.89 \pm .0
‘liv’	ATISS [27]	32.26 \pm .1	1.48 \pm .0	<u>0.71</u> \pm .3	63.87 \pm 6.9	11.43 \pm 3.8	75.30 \pm 5.8	0.58 \pm .0
	Mi-Diff [17]	33.30 \pm .3	1.53 \pm .0	1.06 \pm .2	43.88 \pm 7.6	12.87 \pm 1.4	56.75 \pm 8.8	0.56 \pm .0
	ReSpace/L	<u>31.94</u> \pm .1	<u>1.41</u> \pm .0	<u>0.24</u> \pm .1	<u>24.64</u> \pm 7.8	7.36 \pm 0.4	<u>32.00</u> \pm 7.8	<u>0.84</u> \pm .0
	ReSpace/A [†]	31.90 \pm .2	1.40 \pm .0	0.19 \pm .2	11.20 \pm 3.1	<u>8.22</u> \pm 1.0	19.41 \pm 4.1	0.87 \pm .0
‘all’	ATISS [27]	36.40 \pm .0	1.77 \pm .0	0.22 \pm .1	121.66 \pm 8.6	<u>14.48</u> \pm 1.0	136.14 \pm 8.7	<u>0.57</u> \pm .0
	Mi-Diff [17]	<u>36.14</u> \pm .2	<u>1.72</u> \pm .0	<u>0.07</u> \pm .1	<u>40.51</u> \pm 5.5	18.19 \pm 0.6	<u>58.70</u> \pm 4.9	0.56 \pm .0
	ReSpace/A [†]	35.71 \pm .4	1.67 \pm .0	-0.03 \pm .1	13.11 \pm 3.7	8.67 \pm 2.3	21.78 \pm 6.0	0.87 \pm .0

synthesis. Both models take a 256×256 top-down orthographic projection of the floor plan as an input condition. We use the released source code, modify the pre-processing to fit our custom dataset splits, and re-train all models from scratch on our three different datasets. We do not modify their hyperparameter choice and pick the best model based on their lowest validation loss. We further map the prompt from each instruction to the corresponding ground-truth class label. ATISS is already autoregressive, and single object-addition via one-hot class label conditioning is natively supported. For Mi-Diff, we follow their masking strategy and enable de-noising only for a single object. ATISS and Mi-Diff are chosen since they can be conditioned on non-rectangular floor plans, making them strong baselines for conditional object addition and full scene synthesis. For consistent comparison, we use greedy asset selection for ours, and show details on stochastic selection in Appendix A.3.

Evaluation Metrics. As the main quantitative measure of scene quality, we use our introduced Voxelization-Based Loss (VBL) (see Section 3.3). We follow previous work [27, 21, 17] and render a top-down projection for each scene, computing Fréchet Inception Distance (FID) [15], FID_{CLIP} [19], and Kernel Inception Distance (KID) [3] between the train split and the set of generated scenes. For train splits, we compute a set of $\min(N, 5000)$ renderings for full scenes and single instructions (partial scenes) respectively. We also report Prompt Matching Score (PMS) as a metric measuring how many words w_j from the prompt p_i are captured via the description d_i of the *sampled* 3D asset:

$$\text{PMS}(p_i, d_i) = \frac{1}{|p_i|} \sum_{w_j \in p_i} \mathbb{1}_{w_j \in d_i} \quad (4)$$

Higher recall indicates better prompt matching, directly measuring instruction-following capabilities. For ours, we use the postfixes ‘/B’, ‘/L’, and ‘/A’ to denote the training set for SG-LLM, and denote with ReSpace/A[†] the model with an additional preference alignment stage.

4.2 Prompt-Driven Scene Editing

Object Addition. We present experimental results for object addition (placing a single object into an empty or partial scene) in Table 1, reporting the *delta* VBL to quantify layout changes after insertion. Our method consistently outperforms existing baselines on all reported metrics across all three datasets. Notably, the model trained on ‘all’ (+GRPO) performs stronger even on ‘bed’ and ‘liv’ subsets, indicating that more diverse training scenes and our preference alignment method effectively boost performance, though the latter does not consistently outperform the SFT baseline on the MBL metric. Figure 5 shows qualitative results, with our method performing strongly, sometimes exceeding ground-truth placements (e.g., third row, where the black sofa better matches the prompt and aligns well between side tables). The last row demonstrates a failure case with a bed placed outside scene boundaries for our method as well. However, our method has significantly stronger performance on OOB metrics, empirically validating that an explicit boundary representation seems

Table 2: Quantitative evaluation on **full scenes** on a hold-out test set of 500 unseen floor plans. Each method is trained on the same train splits. For each sample, we use 3 random seeds for full scene generation. KID and Layout Violation (OOB, MBL, VBL) are multiplied by 10^3 for readability.

Method	Scene Renderings			Layout Violations			Prompting	
	\downarrow FID	\downarrow FID _{CLIP}	\downarrow KID $\times 1e3$	\downarrow OOB $\times 1e3$	\downarrow MBL $\times 1e3$	\downarrow VBL $\times 1e3$	\uparrow PMS	
‘bed’	ATISS [27]	43.51 \pm .3	2.34 \pm .1	2.51 \pm .5	414.3 \pm 23.6	99.7 \pm 6.4	514.1 \pm 24.4	n/a
	Mi-Diff [17]	43.18 \pm .4	2.23 \pm .1	1.34 \pm .2	360.1 \pm 18.0	66.6 \pm 9.5	427.0 \pm 08.5	n/a
	ReSpace/A [†]	44.77 \pm .2	2.70 \pm .0	2.17 \pm .1	67.4 \pm 07.1	140.7 \pm 20	208.1 \pm 13.4	0.72 \pm .0
‘liv’	ATISS [27]	44.14 \pm .3	2.26 \pm .0	8.06 \pm .3	506.6 \pm 22.2	135.1 \pm 6.1	641.6 \pm 28.2	n/a
	Mi-Diff [17]	40.76 \pm .1	2.11 \pm .1	4.29 \pm .1	361.5 \pm 12.7	117.1 \pm 3.2	478.7 \pm 09.6	n/a
	ReSpace/A [†]	46.17 \pm .3	2.42 \pm .1	8.05 \pm .7	254.4 \pm 14.2	310.4 \pm 13	564.8 \pm 25.8	0.73 \pm .0
‘all’	ATISS [27]	45.58 \pm .1	2.37 \pm .0	3.87 \pm .1	631.4 \pm 12.9	108.5 \pm 6.9	739.8 \pm 19.0	n/a
	Mi-Diff [17]	42.57 \pm .3	2.14 \pm .0	1.27 \pm .2	327.4 \pm 41.3	87.1 \pm 2.7	414.5 \pm 41.6	n/a
	ReSpace/A [†]	44.85 \pm .2	2.43 \pm .2	2.44 \pm .5	160.2 \pm 16.0	181.6 \pm 26	341.8 \pm 17.9	0.71 \pm .0



Figure 6: Qualitative results on full scene synthesis. For ours, we take results from ReSpace/A[†].

superior to fixed-resolution floor plan renderings as layout complexity beyond rectangular floor plans increases.

Object Removal. We additionally experiment with object removal using the same instructions from the test set. For this, we re-merge the intended object for addition (ground-truth) with the existing scene and prompt the system to *remove* the object given solely the object prompt. As scenes can contain multiple objects of the same asset, they will share the same description d_i . This can lead to ambiguity if only given a short object-level prompt. We treat a removal as correct if all assets matching the prompt 1:1 were removed from the scene and report accuracy as (# correct/# all), with 90.9% \pm 0.6 on ‘bed’, 75.2% \pm 1.0 on ‘liv’, and 87.3% \pm 0.7 on ‘all’.

4.3 Prompt-Driven Full Scene Synthesis

In addition to object-level editing, we evaluate full scene synthesis by conditioning the same models as in Table 1 on empty test set floors. Unlike baselines trained end-to-end on complete scenes, our method relies on prompts from the zero-shot LLM (Figure 2). To improve synthesis quality and the object selection, we inform the LLM with three priors: (1) the complete set of 3D-FRONT object classes, (2) a floor area to object count histogram for appropriate density sampling, and (3) few-shot examples of prompt lists from similar training scenes. Results in Table 2 show we cannot fully outperform baselines across all metrics, excelling mainly on OOB with strong total VBL—confirming that explicit boundaries via SSR are beneficial here as well. Our approach faces two limitations: the zero-shot LLM acts as a bottleneck since it was not trained specifically for this task, and we fix the number of objects based on floor area, without updating prompts after placement, occasionally resulting in cluttered scenes. Figure 6 shows qualitative samples, with large diversity on same floor plans across different methods. For ours, we further have slightly higher numbers for FID/KID metrics. We argue this distribution gap may actually be desirable, offering more diverse arrangements than the dataset alone. Additional samples and failure cases are shown in Appendix A.4.

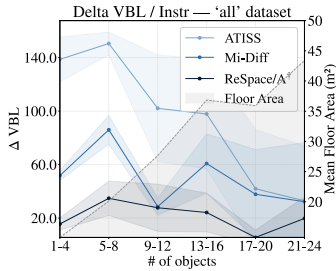


Figure 7: Delta VBL vs. # of objects. Ours is superior with more uniform performance.

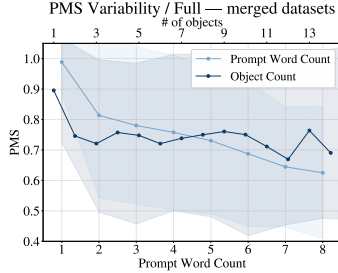


Figure 8: PMS vs. prompt word and object count, with (slight) negative correlation for both.

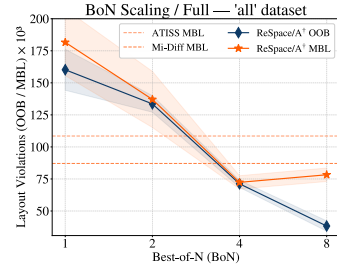


Figure 9: Test-Time Scaling via BoN, showing we can outperform baselines on MBL too.

4.4 Ablations and Discussion

Number of Objects vs. Delta VBL. We study the effect of room size (via floor area) and existing object count on the object addition performance by clustering the number of objects per scene after object addition and aggregating them into uniform bins. We show mean and variance of each bin for the ‘all’ test set in Figure 7 alongside floor area size in light gray. On the one hand, there is a natural positive correlation between increased floor area and higher object count, as there is more free space to choose from for object placement. On the other hand, spatial reasoning complexity can increase substantially for higher object count (regardless of room size). We argue that an ideal model has uniform performance across varying object count, floor area, and scene density. We can see that our method performs much stronger compared to the baselines in this regard.

Prompt Matching Score Variability. To study the impact of prompt-complexity on object addition, we take the prompts that the zero-shot LLM generated for each added object for full scenes and aggregate them by word count and PMS for each uniform bin. We show results on all test sets in Figure 8. Longer prompts involve more complex instructions with more constraints (e.g., SG-LLM needs to satisfy color, material, shape, and style all at the same time). Thus, a negative correlation is naturally expected and confirmed by decreasing PMS with longer word count. We show PMS against number of objects on the same plot with separate x-axis, with slight negative correlation on increased object count as well. This shows that once the scene gets filled up with more objects, it seems harder for SG-LLM to satisfy semantic constraints consistently as it might fall back to priors or other biases.

Scaling Test-Time Compute. We explore Best-of-N (BoN) sampling to demonstrate that SG-LLM captures high-quality placement capabilities that are not consistently sampled. For each object addition, we sample N responses, selecting the optimal one by first filtering candidates with highest PMS (instruction-following), then choosing the one with lowest delta VBL (minimal layout violations). Figure 9 shows results for $N = \{1, 2, 4, 8\}$ on the ‘all’ split. Both OOB and VBL decrease with larger candidate pools, eventually *surpassing* state-of-the-art for MBL on full scene synthesis. The effectiveness of BoN serves as evidence that although GRPO improves upon SFT-only for single object addition, the probability for sampling strong candidates is still lower than optimal. Our approach uniquely benefits from verifiable rewards via geometric constraints (L2 distance on bounding box size), semantic constraints (PMS or SigLIP similarity), and our novel VBL—though the scaling trends observed suggest potential for further advances in preference alignment.

5 Conclusion

We introduced RESPACE, a framework for text-driven 3D indoor scene synthesis using autoregressive language models. Our structured scene representation encodes explicit boundaries and positioning alongside textual descriptions for objects, while our specialized SG-LLM, trained via SFT+GRPO, surpasses state-of-the-art on object addition. By leveraging a zero-shot LLM for object removal and prompt generation, we demonstrate competitive results for full scene synthesis without end-to-end training. This paradigm opens several promising research directions: developing a single model that handles all scene synthesis tasks while maintaining prompt-following capabilities; exploring scaling laws with larger context windows and model size as more training data can be made available; and investigating advanced test-time compute techniques like Monte Carlo Tree Search to optimize full scene synthesis using PMS and VBL rewards directly instead of ‘greedy’ addition.

A Appendix

This Appendix provides the following:

- Details on the preprocessing of the 3D-FRONT dataset, instruction generation, and the creation of our SSR-3DFRONT dataset (Section A.1),
- Implementation details for training our SG-LLM (Section A.2),
- Details on stochastic asset sampling with qualitative results (Section A.3),
- Additional qualitative samples for full scene generation (Section A.4),
- Example of full SSR instance (Section A.5), and
- Prompts for zero-shot LLM for command decomposition and object removal (A.6).

A.1 Dataset Preprocessing for SSR-3DFRONT

Our training data curation is based on the 3D-FRONT [12] dataset, which includes $\sim 19\text{K}$ synthetic indoor scenes of varying size and density, alongside positioned objects referenced from 3D-FUTURE [13], a furniture asset catalog providing textured 3D meshes and renderings for each asset. In order to bring the scenes from the 3D-FRONT dataset [12] into our Structured Scene Representation (SSR), we proceed as follows: First, we leverage an existing dataset of postprocessed 3D room meshes from 3D-FRONT from [8] that has simplified wall geometry and closed holes, which facilitates the room boundary extraction. We run a custom line search algorithm (pseudo-code shown in Algorithm 1) on each room mesh to extract an ordered set of 3D vertices forming a rectilinear polygon for the floor and ceiling. These set of vertices build the room boundaries \mathcal{B}_{top} and $\mathcal{B}_{\text{bottom}}$. Next, we convert the scenes into JSON, resembling our proposed SSR (see Section 3.1). We define 3 room types: ‘bedroom’ for bedrooms, ‘livingroom’ for living rooms, dining rooms and living/dining rooms, and ‘other’ for all remaining rooms. We only consider scenes that have valid scene boundaries with $|\{b_i\}| \geq 4$, an object count of $3 \leq |\{o_i\}| \leq 50$, and $\text{VBL} < 0.1$. The latter filters out “invalid” scenes that contain too many object or boundary collisions (see Section 3.3). Since a few scenes have only a single malpositioned object, we further check for scene validity if a single object already violates this filter (via $\text{VBL} \geq 0.1$), and keep the modified scene if removing that object makes the scene valid. We shift all scenes to the origin $(0, 0, 0)$. In total, this results in 13055 valid scenes after preprocessing. “SSR-3DFRONT” is available via huggingface.co/datasets/gradient-spaces/SSR-3DFRONT

Algorithm 1 Rectilinear Polygon Corner Extraction

Require: Mesh vertices $V \in \mathbb{R}^{n \times 3}$

Ensure: Corner vertices C forming rectilinear polygon

```
1:  $P \leftarrow \text{unique}(V[:, [0, 1]])$  ▷ Project to unique 2D points
2:  $(x_0, y_0) \leftarrow \arg \min_{v: v_x = \min(P[:, 0])} v_y$ ,  $\text{dir} \leftarrow \text{'north'}$ ,  $\text{curr} \leftarrow (x_0, y_0)$ ,  $C \leftarrow []$ 
3: repeat
4:    $S \leftarrow \text{getSortedAxisPoints}(P, \text{curr}, \text{dir})$  ▷ Points on same axis, sorted by direction
5:    $i \leftarrow \text{indexOf}(\text{curr}, S) + 1$ 
6:   while  $\neg \text{isCornerPoint}(P, S[i], \text{dir})$  do  $i \leftarrow i + 1$ 
7:   end while
8:    $\text{curr} \leftarrow S[i]$ ,  $\text{dir} \leftarrow \text{getNextDirection}(P, \text{curr}, \text{dir})$ ,  $C.append(\text{curr})$ 
9: until  $\text{curr} = (x_0, y_0)$ 
10: return  $C$ 
```

A.1.1 Prompts for Asset Description and Prompt Bank

As mentioned in Section 4, the raw 3D-FRONT dataset does not contain textual descriptions of assets or scenes, and we leverage GPT-4o [18] as a Vision-Language Model (VLM) to generate sentence-level descriptions d_j for each object o_j in the catalog. We query the VLM by attaching a rendering of the asset with a prompt that includes the provided class label. After obtaining sentence-level descriptions for each generation, we leverage the same VLM to generate 10 unique, concise prompts (2-5 words in noun phrase format) for each asset description d_j . This approach serves two purposes: (i) it covers diverse prompting styles with varying levels of detail and word order, and (ii)

it prevents trivial overfitting on our small dataset by avoiding repetition of identical prompts that lead to memorization rather than generalization. We provide the full prompt for extracting visual properties in textual form for each asset in the 3D-FUTURE dataset [13] in Figure 10 and for prompt generation in Figure 11. For asset descriptions, we leverage the content provided in the ‘summary’ as it seemed to best capture dense semantics that refer to style, color, material, etc.

User Prompt
Please provide a concise JSON object of the furniture item in the image using ‘style’, ‘color’, ‘material’, ‘characteristics’, and ‘summary’ as keys. Describe the style, noting any blends of design elements. Specify the materials used for different components (if applicable). List the key characteristics, including the shape, design features, and any distinctive elements or decorative accents. If there are multiple values for a key, use a list of strings. DO NOT build a nested JSON. The summary compactly captures the essence of the furniture’s style, functionality, and aesthetic appeal, emphasizing its unique attributes. This description should clearly differentiate this piece from others while succinctly capturing its essential properties and we will use it for object retrieval, so it should be as accurate as possible, keyword-heavy, but just be one extremely short sentence. You are an interior designer EXPERT. Hint: It’s a {ASSET_OBJECT_CATEGORY_LABEL}. Only output the JSON as a plain string and nothing else.

Figure 10: Prompt for GPT-4o[18] for extracting various object properties for each asset including a sentence-level asset description, given a rendering of an object in the 3D-FUTURE dataset [13].

User Prompt
The list below contains a sentence referring to a single piece of furniture. Your task is to create a list of 10 short descriptions that vary in length. Each description refers to the subject with a maximum of 3-4 additional descriptive words that reference the color, style, shape, etc. All your sentences should be in ‘noun phrase’. You MUST include a variety of lengths in your descriptions, ensuring a few samples are very short (1-2 words max) and others are longer (4-5 words). Have at least one sample with only one word, except if you need to be more specific for the subject, e.g., use ‘Coffee Table’, not just ‘Table’, if present. Use mostly basic properties such as color or material, but also include a few creative and diverse versions to increase robustness in our ML training dataset.
The sentence is:
- {ASSET_DESCRIPTION}
Just output a plain list and nothing else. You have only one list of 10 descriptions. You MUST always point to the referenced object above and not hallucinate other furniture or be overly generic by using ‘furniture’ or ‘piece’. Every list contains the descriptions in increasing word length. Just output the final JSON object as a plain string without any key. Never use markdown or ``json`.

Figure 11: Prompt for GPT-4o[18] for generating a prompt bank with a list of 10 unique prompts, given a sentence-level asset description.

A.1.2 Instruction Generation for SG-LLM

Given the full scenes, we impose dynamic instruction generations based on a stochastic recipe. Let $\mathcal{P}(o) = \{p_1, \dots, p_K\}$ be the fixed prompt bank for object o (we set $K = 10$). During training, we turn \mathcal{S} into an instruction tuple: $\mathcal{I} = (\hat{\mathcal{S}}, p, o_{\text{add}})$, where the model must learn to add object o_{add} to the partial scene $\hat{\mathcal{S}} = (\mathcal{T}, \mathcal{B}, \hat{\mathcal{O}})$ when conditioned on the natural-language prompt p . To generate a tuple, we first draw a random permutation for the order of objects $\pi \sim \text{Unif}(S_N)$, then uniformly sample the prompt $p \sim \text{Unif}(\mathcal{P}(o_{\text{add}}))$ for object o_{add} . Let $Z \in \{Z_0, Z_1, Z_2\}$ be the instruction type: Z_0 (‘zero_start’), Z_1 (‘full_scene’), and Z_2 (‘random’), with Z_0 teaching the model to start from an empty room given only the prompt, Z_1 teaching ‘scene completion’ as the final contains all objects from the scene but o_{add} , and Z_2 teaching robust object placements on arbitrary, shuffled partial scenes. For Z_0 we set $\hat{\mathcal{O}} = \emptyset$, $o_{\text{add}} = o_{\pi(1)}$. For Z_1 we set $\hat{\mathcal{O}} = \{o_{\pi(1)}, \dots, o_{\pi(N-1)}\}$, $o_{\text{add}} = o_{\pi(N)}$. For Z_2 we draw a drop count $M \sim \text{Unif}\{0, \dots, N - 1\}$, put $L = N - M$ and define $o_{\text{add}} = o_{\pi(L)}$, $\hat{\mathcal{O}} = \{o_{\pi(1)}, \dots, o_{\pi(L-1)}\}$. Instruction type is sampled as $Z \sim \text{Cat}(w_0, w_1, w_2)$ with fixed $w_0 = w_1 = 0.1$, $w_2 = 0.8$ and the conditional distribution factorizes as

$$p(\mathcal{I} | \mathcal{S}) = \sum_{z=0}^2 w_z p(\mathcal{I} | Z = z, \mathcal{S}),$$

$$p(\mathcal{I} | Z = z, \mathcal{S}) = \begin{cases} \frac{\mathbf{1}_{\{z=0\}}}{N |\mathcal{P}(o_{\text{add}})|} & (z = 0), \\ \frac{\mathbf{1}_{\{z=1\}}}{N! |\mathcal{P}(o_{\text{add}})|} & (z = 1), \\ \frac{\mathbf{1}_{\{z=2\}}}{N! N |\mathcal{P}(o_{\text{add}})|} & (z = 2) \end{cases}$$

Thus, for Z_2 , we choose one of $N!$ permutations, one of N drop counts, and one of $|\mathcal{P}(o_{\text{add}})|$ prompts. Fixed weights $w_0 = w_1 = 0.1$ guarantee at least 20% exposure to the empty-room and

near-complete-room edge cases even for very large scenes. Since we have empty or full scenes with $\frac{1}{N}$ probability (and partial scenes otherwise), their likelihood decreases inversely proportional with higher object count. Imposing minimum exposure via fixed weights ensures the model learns these edge cases as well. We perform random data augmentation on train/val samples by (i) rotating each scene by $\theta \in \{0, 90, 180, 270\}^\circ$, (ii) cyclically shifting room bounds in a round-robin fashion, and (iii) slightly perturbing x - and z -components of every position and size vector of each object with a uniform delta with $v' = v + \delta$ and $\delta \sim U(-0.02, 0.02)$ for coordinate values v .

A.2 Implementation Details for SG-LLM

We trained SG-LLM on 4xA100 NVIDIA 80GB GPUs and a system with 16 available CPUs with 384GB RAM. We used Python 3.9.0 with CUDA 12.1.1 and GCC 10.3.0, and ‘bf16’ for numerical precision with a local batch size of 4 and a gradient accumulation step (GAS) of 8. For the first stage, we perform Supervised Fine-Tuning (SFT) on the full weights for 30-50 hours with a learning rate (LR) of 5e-5 and choose the model with best validation loss via mean delta VBL on the val split. We use a context window of 3000 tokens. We further experimented with Low-Rank Adaptation (LoRA) [16] but observed faster convergence with SFT on full weights. For GRPO fine-tuning, we use an LR of 5e-5, temp = 0.7, batch size of 4, GAS of 16, and 4 generations per sample/instruction. We train the latter for around 30 hours and pick the model based on best delta VBL. For SFT, this resulted in the best model at around 70 epochs, for GRPO at around 3 epochs. For GRPO, we observed instability with higher LRs (>5e-5) and without excluding candidates with valid JSONs but object properties that do not pass the filter used in Section 4.1. High-quality samples (w.r.t. filtering) only appear with around 25% probability, and we suspect that the negative rewards corrupt the SFT behavior too aggressively (especially the JSON structure). Further, without our strong filter for high-quality samples, we observed reward hacking via GRPO: the model produced valid JSONs but found a way to optimize description and size such that smaller objects got placed, effectively reducing the probability of intersections and decreasing the VBL. However, as this is not a desired behavior, we imposed a stronger filter for positive rewards. Future work can investigate the trade-offs between LR, reward shaping, and reward distribution.

A.3 Stochastic Asset Sampling

Our proposed stochastic asset sampling involves various hyperparameters to tweak the final discrete distribution. We heuristically found that $\lambda = 0.5$, $\sigma = 0.2$, temp = 0.2, top_p = 0.95, and top_k=20 perform the best. However, for all experiments reported in the results of the main paper (see Section 4), we impose a *greedy selection* strategy for asset sampling in order to maintain better comparison with baselines. We use the same hyperparameters as above and choose the top-1 asset via $\text{argmax}_{m_j} g_\phi(d_i, h_i)$. For comparison, we show true asset sampling (with the same hyperparameters) in Figure 12 on the same instructions from Figure 5 and 3 randomly sampled assets. We can simply sample from the distribution (instead of top-1 selection) for true stochasticity. We suggest that there might not be a single set of best hyperparameters for asset sampling. Instead, the user might tweak λ , (i.e., the strength of the semantic embedding), or σ (i.e., the sharpness of the size matching via 3D bounding boxes) dynamically during scene generation to guide the process towards more desired candidates. With $\lambda = 0.5$, both geometry (via 3d bounding box size differences) and semantics (via SigLIP embeddings) have equal contribution to the final distribution for samples picked in Figure 12.

A.4 More Qualitative Examples on Full Scenes

In Figure 13, we show additional qualitative samples for full scene synthesis (with greedy asset sampling; otherwise same setup as done in the main experiments in Section 4). In contrast to Figure 6 where we showed the empty floor plan on the very left, we omit that column and replace it with Best-of-N (BoN) results from our method with BoN=8 on the very far right column. Due to the inherent randomness in our full pipeline between different BoN runs (i.e., especially involving the zero-shot LLM for the prompt list generation and the sampling of few shot samples and number of objects via priors), results for ours with BoN=1 and BoN=8 do not consistently involve the same object prompt lists into SG-LLM (i.e., 2nd column or 2nd to last column contain different scene-level compositions). Despite this fact, the BoN=8 results show superior performance compared to BoN=1, with less OOB and MBL, and better overall composition.

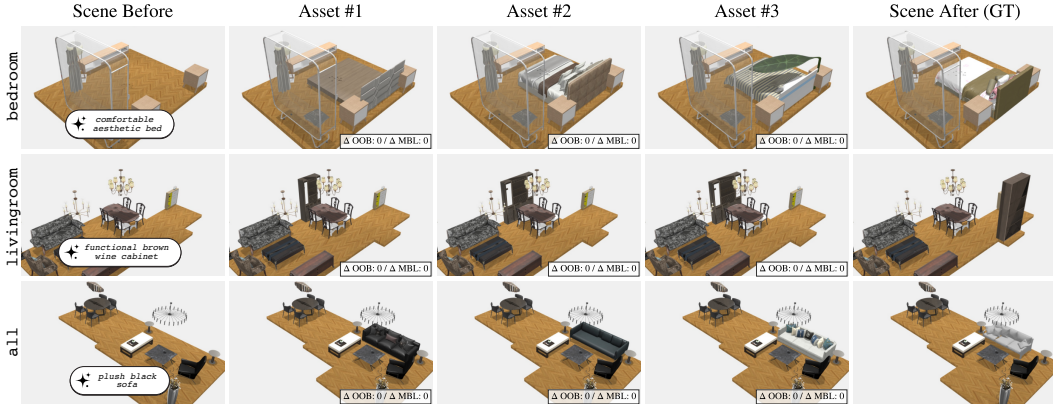


Figure 12: Qualitative results for true stochastic asset sampling without greedy selection (as done for the samples shown in Figure 5).

A.5 Example of Full SSR Instance

We show a full example of a Structured Scene Representation (SSR) instance with sampled assets in Listing 1. The “abstract” SSR—before concrete 3D asset selection—would simply not contain the key/value pairs with ‘sampled_’ prefix and the optional ‘uuid’ key/value pair, as they are added after asset selection. For numerical values, we omit ‘pretty formatting’ (with line breaks after every element) in order to fit the example into a single page in this PDF.

Listing 1: Example of SSR instance with sampled assets

```

1 {
2   "room_type": "bedroom",
3   "bounds_top": [[-1.55, 2.6, 1.9], [1.55, 2.6, 1.9], [1.55, 2.6,
4     -1.9], [-1.55, 2.6, -1.9]],
5   "bounds_bottom": [[-1.55, 0.0, 1.9], [1.55, 0.0, 1.9], [1.55, 0.0,
6     -1.9], [-1.55, 0.0, -1.9]],
7   "objects": [
8     {
9       "desc": "A contemporary king-size bed with a brown padded
10        headboard, Hello Kitty-themed pink and white bedding,
11        graphic pillows, and bolster cushions, offering a playful
12        yet comfortable aesthetic",
13       "size": [ 1.77, 0.99, 1.94 ],
14       "pos": [ 0.44, 0.0, -0.44 ],
15       "rot": [ 0.0, 0.70711, 0.0, -0.70711 ],
16       "jid": "8a31d51c-2306-439f-90c6-650be7284975",
17       "sampled_asset_jid": "7bf721bf-8839-4343-95c5-b6e852805ad1
18         -(0.83)-(1.0)-(0.86)",
19       "sampled_asset_desc": "Modern minimalist king-size bed with a
20         wood frame, padded gray fabric headboard, and clean lines.",
21       "sampled_asset_size": [1.77, 1.02, 2.03],
22       "uuid": "d3d31dbc-ff1d-4122-8a80-52598c326f00"
23     },
24     ...
25   ]
26 }

```

A.6 Prompts for Zero-Shot Model

The full prompt for user instruction decomposition is in Figure 14. We further show an example of input/output prompts for a full scene generation in Figure 15. The prompt for object removal, using the same zero-shot LLM, is shown in Figure 16, with an example of input/output in Figure 17.

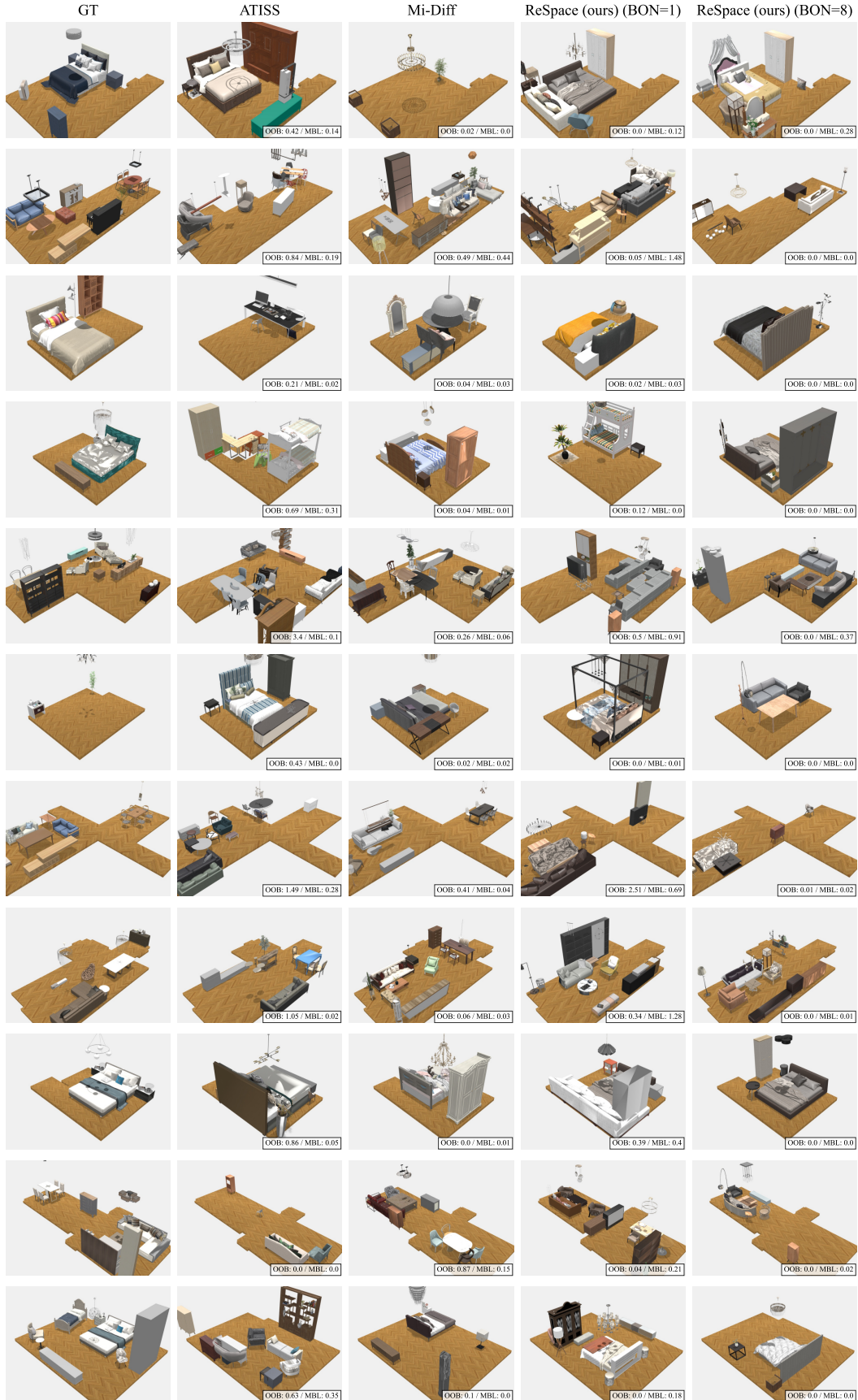


Figure 13: Qualitative results (random selection) on full scene synthesis compared with baselines. For ours, we show both BoN=1 and BoN=8.

```

System Prompt
you are a world-class leading interior design expert. your task is to fulfill the request of the user
about interior design but you have help of another world-class expert model that can only be called in an
XML-style API.
# input
- <prompt> : the user request
- <scenegraph> : the current scene will be given as a JSON object. in some cases, there will be no scene
graph given, which means there is no "current" scene to work with. the "bounds_top" and "bounds_bottom"
keys contain the boundaries as a list of 3D vertices in metric space.
# task
- composing a list of commands to fulfill the user request via <add> and <remove> commands. ideally, you
reflect the existing objects in the scenegraph, if one is given.
# adding
- if the user wants to add one or multiple objects, you create an <add> command for every object/furniture
and add it to the list in "commands".
- for the description, you should refer to the subject with a maximum of five additional descriptive
words. the first words should refer to the color / style / shape / etc., while the last word should
always be the main subject. your description must be in 'noun phrase'.
- if the user request provides an existing scene description provided via <scenegraph>...</scenegraph>
and there are existing objects in the scene, you should try to match the style of the existing objects by
providing a similar style as part of the description of your commands.
- if the user provides some requirement about particular furniture that should be present in the room, you
should always add these objects via <add> commands.
- your format should be: <add>description</add>
- DO NEVER use more than 5 words for each description
# removing / swapping
- if the user wants to remove one to multiple objects, you add a <remove> command for every object that
should be removed.
- if the user wants to swap or replace furniture, you MUST use <remove> first and then use <add>
- if there are similar candidates for removal you should remove the object that matches the description
best.
- your format should be: <remove>description</remove>
- you can keep the description short here as well
# output
- the commands are given as a list under the "commands" key where each command follows EXACTLY the format
specified above and is given as a string, i.e. "<add>...</add>" or "<remove>...</remove>".
- if there are remove commands, you always put them BEFORE add commands.
- IMPORTANT: you NEVER use the <remove> commands unless the user EXPLICITLY asks for it via swapping or
removing objects. you do not make assumptions about this.
- you NEVER remove objects to "match the style" or if there is already an object in the scene similar
to the requested one. a scene can contain as many similar objects as the user wants. you ONLY remove
objects if the user explicitly asks for removal or swapping.
- if you use the <remove> command, you MUST provide your reasoning under the "reasoning" key, which comes
before the "commands" key in the same JSON object. - you always output the final JSON object as a plain
string and nothing else. NEVER use markdown.
# available object classes
- you should only pick objects for <add> based on the following high-level abstract classes
- your objects should be more specific than these classes but you should not add objects that are not part
of these classes/labels
{UNIQUE_OBJECT_CLASSES}
# available object classes
- you should only pick objects for <add> based on the following high-level abstract classes
- your objects should be more specific than these classes but you should not add objects that are not part
of these classes/labels
# few-shot examples for scenes that have a similar size to the requested one (your scene should be
different though and stick to the user prompt):{PROMPT_LISTS_FOR_K_EXAMPLES}
REMINDER: each description in your <add>...</add> commands should be IN NOUN PHRASE WITH 2-3 words AND AT
MAXIMUM 5 words

```

```

User Prompt
<prompt>{UNSTRUCTURED_USER_INSTRUCTION}</prompt>
<scenegraph>{JSON_DUMP_OF_SSR_IF_PROVIDED_OR_NONE}</scenegraph>

```

Figure 14: System and User Prompt for the zero-shot LLM for command decomposition.

```

User Prompt
<prompt>create a bedroom with 5 objects.</prompt> <scenegraph>"room_type": "bedroom", "bounds_top":
[[-3.2, 2.65, 1.7], [3.2, 2.65, 1.7], [3.2, 2.65, -0.1], [0.9, 2.65, -0.1], [0.9, 2.65, -1.7], [-3.2,
2.65, -1.7]], "bounds_bottom": [[-3.2, 0.0, 1.7], [3.2, 0.0, 1.7], [3.2, 0.0, -0.1], [0.9, 0.0, -0.1],
[0.9, 0.0, -1.7], [-3.2, 0.0, -1.7]], "objects": []</scenegraph>

```

```

Response (Model Output)
'commands': ['<add>dark wooden double bed</add>', '<add>creamy white nightstand</add>', '<add>black floor
lamp</add>', '<add>white two-seat sofa</add>', '<add>low shelf</add>']

```

Figure 15: Example of an input/output pair to the zero-shot LLM on full scene synthesis. Each command gets iteratively processed by ReSpace. For full scene synthesis, this results in an autoregressive loop into SG-LLM such that objects get added into the partial scene.

```

System Prompt
you are a world-class leading interior design expert. your task is to remove furniture given the
descriptions in the header and the current list of furniture in the body. you must respond ONLY with a
valid JSON string that matches precisely the *format* of the existing JSON in the request.
if there are multiple objects that match the description precisely, you should remove all of them.
the prompt for the object to be removed will be given in the header between <remove>...</remove> tags.
the current scene will be given as a JSON object in the body between <scenegraph>...</scenegraph> tags.
in the successful case, your output contains one or N fewer objects in the "objects" list and the rest of
the JSON object should be EXACTLY identical to the input.
you can also remove all objects if the prompt matches those objects. in that case, you provide an empty
list for the "objects" key.
you can further assume that in most cases, there will be at least one object in the scene that matches
the description roughly. this object shall be removed.
only output the JSON (with the removed objects) as a plain string and nothing else.

User Prompt
<remove>{OBJECT_PROMPT_FOR_REMOVAL}</remove>
<scenegraph>{JSON_DUMP_OF_SSR}</scenegraph>

```

Figure 16: System and User Prompt for the zero-shot LLM for object removal.

```

User Prompt
<remove>comfortable aesthetic bed</remove>
<scenegraph>{"room_type": "bedroom", "bounds_top": [[-1.55, 2.6, 1.9], [1.55, 2.6, 1.9], [1.55, 2.6,
-1.9], [-1.55, 2.6, -1.9]], "bounds_bottom": [[-1.55, 0.0, 1.9], [1.55, 0.0, 1.9], [1.55, 0.0, -1.9],
[-1.55, 0.0, -1.9]], "objects": [{"desc": "Mid-Century Modern nightstand with light wood finish,
geometric cutout handle, and angled legs.", "size": [0.5, 0.55, 0.43], "pos": [1.37, 0.0, -1.45],
"rot": [0, -0.70711, 0, 0.70711], "jid": "9603344b-99b8-43db-abf0-73c7eaf0ea5f-(0.81)-(1.0)-(0.72)",
"desc": "Modern minimalist TV stand with walnut brown wood, white accents, two closed cabinets, and
open shelving on raised legs.", "size": [1.86, 0.42, 0.35], "pos": [-1.35, 0.0, -0.52], "rot": [0,
0.70711, 0, 0.70711], "jid": "18d54650-68ae-4d4b-8079-1f050b267153-(1.01)-(1.0)-(0.82)", "desc":
"Modern industrial wardrobe with a minimalist metal and mesh design, featuring a rectangular shape,
four slender legs, a single shelf, and a hanging rod.", "size": [1.6, 2.11, 0.5], "pos": [0.74,
0.0, 1.56], "rot": [0, 1, 0, 0], "jid": "19035101-21a1-4495-ae95-90d8d1ccd108-(1.55)-(1.0)-(1.04)",
"desc": "Modern minimalist floor lamp with a white fabric drum shade and brown wooden tripod base
featuring an open geometric design.", "size": [0.47, 1.1, 0.47], "pos": [-1.27, 0.0, 0.6], "rot":
[0, -0.35334, 0, 0.93549], "jid": "4e086af8-0900-4c6d-b535-08c7a936a981-(1.0)-(0.85)-(1.0)",
"desc": "Modern adjustable pendant lamp with branching black metal arms, gold disk shades,
and minimalist design.", "size": [0.36, 1.03, 0.32], "pos": [0.06, 1.79, -0.13], "rot":
[0, 0, 0, 1], "jid": "6289a052-b4a7-417a-b687-b22fddc14663-(0.23)-(1.0)-(0.31)", "desc":
"Mid-Century Modern nightstand with light wood finish, geometric cutout handle, and angled
legs.", "size": [0.5, 0.55, 0.43], "pos": [1.35, 0.0, 0.62], "rot": [0, -0.70711, 0, 0.70711],
"jid": "9603344b-99b8-43db-abf0-73c7eaf0ea5f-(0.81)-(1.0)-(0.72)", "desc": "A contemporary
king-size bed with a brown padded headboard, Hello Kitty-themed pink and white bedding,
graphic pillows, and bolster cushions, offering a playful yet comfortable aesthetic.", "size":
[1.56, 0.9, 2.22], "pos": [0.54, 0.0, -0.43], "rot": [0, -0.70711, 0, 0.70711], "jid":
"bff6e7b4-4e17-401d-b684-dc768def3869-(0.88)-(0.91)-(1.14)"}]</scenegraph>

```

```

Response (Model Output)
"room_type": "bedroom", "bounds_top": [[-1.55, 2.6, 1.9], [1.55, 2.6, 1.9], [1.55, 2.6, -1.9], [-1.55,
2.6, -1.9]], "bounds_bottom": [[-1.55, 0.0, 1.9], [1.55, 0.0, 1.9], [1.55, 0.0, -1.9], [-1.55, 0.0,
-1.9]], "objects": [{"desc": "Mid-Century Modern nightstand with light wood finish, geometric cutout
handle, and angled legs.", "size": [0.5, 0.55, 0.43], "pos": [1.37, 0.0, -1.45], "rot": [0, -0.70711,
0, 0.70711], "jid": "9603344b-99b8-43db-abf0-73c7eaf0ea5f-(0.81)-(1.0)-(0.72)", "desc": "Modern
minimalist TV stand with walnut brown wood, white accents, two closed cabinets, and open shelving
on raised legs.", "size": [1.86, 0.42, 0.35], "pos": [-1.35, 0.0, -0.52], "rot": [0, 0.70711,
0, 0.70711], "jid": "18d54650-68ae-4d4b-8079-1f050b267153-(1.01)-(1.0)-(0.82)", "desc": "Modern
industrial wardrobe with a minimalist metal and mesh design, featuring a rectangular shape, four
slender legs, a single shelf, and a hanging rod.", "size": [1.6, 2.11, 0.5], "pos": [0.74, 0.0,
1.56], "rot": [0, 1, 0, 0], "jid": "19035101-21a1-4495-ae95-90d8d1ccd108-(1.55)-(1.0)-(1.04)",
"desc": "Modern minimalist floor lamp with a white fabric drum shade and brown wooden tripod base
featuring an open geometric design.", "size": [0.47, 1.1, 0.47], "pos": [-1.27, 0.0, 0.6], "rot":
[0, -0.35334, 0, 0.93549], "jid": "4e086af8-0900-4c6d-b535-08c7a936a981-(1.0)-(0.85)-(1.0)",
"desc": "Modern adjustable pendant lamp with branching black metal arms, gold disk shades,
and minimalist design.", "size": [0.36, 1.03, 0.32], "pos": [0.06, 1.79, -0.13], "rot":
[0, 0, 0, 1], "jid": "6289a052-b4a7-417a-b687-b22fddc14663-(0.23)-(1.0)-(0.31)", "desc":
"Mid-Century Modern nightstand with light wood finish, geometric cutout handle, and angled legs.",
"size": [0.5, 0.55, 0.43], "pos": [1.35, 0.0, 0.62], "rot": [0, -0.70711, 0, 0.70711], "jid":
"9603344b-99b8-43db-abf0-73c7eaf0ea5f-(0.81)-(1.0)-(0.72)"}]

```

Figure 17: Example of an input/output pair to the zero-shot LLM on object removal.

References

- [1] Rio Aguina-Kang, Maxim Gumin, Do Heon Han, Stewart Morris, Seung Jean Yoo, Aditya Ganeshan, R Kenny Jones, Qihong Anna Wei, Kailiang Fu, and Daniel Ritchie. Open-universe indoor scene generation using llm program synthesis and uncurated object databases. *arXiv preprint arXiv:2403.09675*, 2024.
- [2] Armen Avetisyan, Christopher Xie, Henry Howard-Jenkins, Tsun-Yi Yang, Samir Aroudj, Suvam Patra, Fuyang Zhang, Duncan Frost, Luke Holland, Campbell Orme, et al. Scenescrypt: Reconstructing scenes with an autoregressive structured language model. In *European Conference on Computer Vision*, pages 247–263. Springer, 2024.
- [3] Mikołaj Bińkowski, Danica J Sutherland, Michael Arbel, and Arthur Gretton. Demystifying mmd gans. *arXiv preprint arXiv:1801.01401*, 2018.
- [4] Bradley Brown, Jordan Juravsky, Ryan Ehrlich, Ronald Clark, Quoc V Le, Christopher Ré, and Azalia Mirhoseini. Large language monkeys: Scaling inference compute with repeated sampling. *arXiv preprint arXiv:2407.21787*, 2024.
- [5] Tom Brown, Benjamin Mann, Nick Ryder, Melanie Subbiah, Jared D Kaplan, Prafulla Dhariwal, Arvind Neelakantan, Pranav Shyam, Girish Sastry, Amanda Askell, et al. Language models are few-shot learners. *Advances in neural information processing systems*, 33:1877–1901, 2020.
- [6] Ata Çelen, Guo Han, Konrad Schindler, Luc Van Gool, Iro Armeni, Anton Obukhov, and Xi Wang. I-design: Personalized llm interior designer. *arXiv preprint arXiv:2404.02838*, 2024.
- [7] Paul F Christiano, Jan Leike, Tom Brown, Miljan Martic, Shane Legg, and Dario Amodei. Deep reinforcement learning from human preferences. *Advances in neural information processing systems*, 30, 2017.
- [8] Manuel Dahnert, Ji Hou, Matthias Nießner, and Angela Dai. Panoptic 3d scene reconstruction from a single rgb image. *Advances in Neural Information Processing Systems*, 34:8282–8293, 2021.
- [9] Helisa Dharmo, Fabian Manhardt, Nassir Navab, and Federico Tombari. Graph-to-3d: End-to-end generation and manipulation of 3d scenes using scene graphs. In *Proceedings of the IEEE/CVF International Conference on Computer Vision*, pages 16352–16361, 2021.
- [10] Weixi Feng, Wanrong Zhu, Tsu-jui Fu, Varun Jampani, Arjun Akula, Xuehai He, Sugato Basu, Xin Eric Wang, and William Yang Wang. Layoutgpt: Compositional visual planning and generation with large language models. *Advances in Neural Information Processing Systems*, 36:18225–18250, 2023.
- [11] Matthew Fisher, Manolis Savva, Yangyan Li, Pat Hanrahan, and Matthias Nießner. Activity-centric scene synthesis for functional 3d scene modeling. *ACM Transactions on Graphics (TOG)*, 34(6):1–13, 2015.
- [12] Huan Fu, Bowen Cai, Lin Gao, Ling-Xiao Zhang, Jiaming Wang, Cao Li, Qixun Zeng, Chengyue Sun, Rongfei Jia, Binqiang Zhao, et al. 3d-front: 3d furnished rooms with layouts and semantics. In *Proceedings of the IEEE/CVF International Conference on Computer Vision*, pages 10933–10942, 2021.
- [13] Huan Fu, Rongfei Jia, Lin Gao, Mingming Gong, Binqiang Zhao, Steve Maybank, and Dacheng Tao. 3d-future: 3d furniture shape with texture. *International Journal of Computer Vision*, 129: 3313–3337, 2021.
- [14] Aaron Grattafiori, Abhimanyu Dubey, Abhinav Jauhri, Abhinav Pandey, Abhishek Kadian, Ahmad Al-Dahle, Aiesha Letman, Akhil Mathur, Alan Schelten, Alex Vaughan, et al. The llama 3 herd of models. *arXiv preprint arXiv:2407.21783*, 2024.
- [15] Martin Heusel, Hubert Ramsauer, Thomas Unterthiner, Bernhard Nessler, and Sepp Hochreiter. Gans trained by a two time-scale update rule converge to a local nash equilibrium. *Advances in neural information processing systems*, 30, 2017.

- [16] Edward J Hu, Yelong Shen, Phillip Wallis, Zeyuan Allen-Zhu, Yuanzhi Li, Shean Wang, Lu Wang, Weizhu Chen, et al. Lora: Low-rank adaptation of large language models. *ICLR*, 1(2):3, 2022.
- [17] Siyi Hu, Diego Martin Arroyo, Stephanie Debats, Fabian Manhardt, Luca Carlone, and Federico Tombari. Mixed diffusion for 3d indoor scene synthesis. *arXiv preprint arXiv:2405.21066*, 2024.
- [18] Aaron Hurst, Adam Lerer, Adam P Goucher, Adam Perelman, Aditya Ramesh, Aidan Clark, AJ Ostrow, Akila Welihinda, Alan Hayes, Alec Radford, et al. Gpt-4o system card. *arXiv preprint arXiv:2410.21276*, 2024.
- [19] Tuomas Kynkäänniemi, Tero Karras, Miika Aittala, Timo Aila, and Jaakko Lehtinen. The role of imagenet classes in fréchet inception distance. In *The Eleventh International Conference on Learning Representations*.
- [20] Nathan Lambert, Jacob Morrison, Valentina Pyatkin, Shengyi Huang, Hamish Ivison, Faeze Brahman, Lester James V Miranda, Alisa Liu, Nouha Dziri, Shane Lyu, et al. Tulu 3: Pushing frontiers in open language model post-training. *arXiv preprint arXiv:2411.15124*, 2024.
- [21] Chenguo Lin and Yadong Mu. Instructscene: Instruction-driven 3d indoor scene synthesis with semantic graph prior. *arXiv preprint arXiv:2402.04717*, 2024.
- [22] Jingyu Liu, Wenhan Xiong, Ian Jones, Yixin Nie, Anchit Gupta, and Barlas Oğuz. Clip-layout: Style-consistent indoor scene synthesis with semantic furniture embedding. *arXiv preprint arXiv:2303.03565*, 2023.
- [23] Andrew Luo, Zhoutong Zhang, Jiajun Wu, and Joshua B Tenenbaum. End-to-end optimization of scene layout. In *Proceedings of the IEEE/CVF Conference on Computer Vision and Pattern Recognition*, pages 3754–3763, 2020.
- [24] Léopold Maillard, Nicolas Sereyjol-Garros, Tom Durand, and Maks Ovsjanikov. Debara: Denoising-based 3d room arrangement generation. *Advances in Neural Information Processing Systems*, 37:109202–109232, 2024.
- [25] Ben Mildenhall, Pratul P Srinivasan, Matthew Tancik, Jonathan T Barron, Ravi Ramamoorthi, and Ren Ng. Nerf: Representing scenes as neural radiance fields for view synthesis. *Communications of the ACM*, 65(1):99–106, 2021.
- [26] Long Ouyang, Jeffrey Wu, Xu Jiang, Diogo Almeida, Carroll Wainwright, Pamela Mishkin, Chong Zhang, Sandhini Agarwal, Katarina Slama, Alex Ray, et al. Training language models to follow instructions with human feedback. *Advances in neural information processing systems*, 35:27730–27744, 2022.
- [27] Despoina Paschalidou, Amlan Kar, Maria Shugrina, Karsten Kreis, Andreas Geiger, and Sanja Fidler. Atiss: Autoregressive transformers for indoor scene synthesis. *Advances in Neural Information Processing Systems*, 34:12013–12026, 2021.
- [28] Songyou Peng, Michael Niemeyer, Lars Mescheder, Marc Pollefeys, and Andreas Geiger. Convolutional occupancy networks. In *Computer Vision—ECCV 2020: 16th European Conference, Glasgow, UK, August 23–28, 2020, Proceedings, Part III 16*, pages 523–540. Springer, 2020.
- [29] Pulak Purkait, Christopher Zach, and Ian Reid. Sg-vae: Scene grammar variational autoencoder to generate new indoor scenes. In *European Conference on Computer Vision*, pages 155–171. Springer, 2020.
- [30] Siyuan Qi, Yixin Zhu, Siyuan Huang, Chenfanfu Jiang, and Song-Chun Zhu. Human-centric indoor scene synthesis using stochastic grammar. In *Proceedings of the IEEE Conference on Computer Vision and Pattern Recognition*, pages 5899–5908, 2018.
- [31] Alec Radford, Jong Wook Kim, Chris Hallacy, Aditya Ramesh, Gabriel Goh, Sandhini Agarwal, Girish Sastry, Amanda Askell, Pamela Mishkin, Jack Clark, et al. Learning transferable visual models from natural language supervision. In *International conference on machine learning*, pages 8748–8763. PmLR, 2021.

- [32] Rafael Rafailov, Archit Sharma, Eric Mitchell, Christopher D Manning, Stefano Ermon, and Chelsea Finn. Direct preference optimization: Your language model is secretly a reward model. *Advances in Neural Information Processing Systems*, 36:53728–53741, 2023.
- [33] Daniel Ritchie, Kai Wang, and Yu-an Lin. Fast and flexible indoor scene synthesis via deep convolutional generative models. In *Proceedings of the IEEE/CVF conference on computer vision and pattern recognition*, pages 6182–6190, 2019.
- [34] Zhihong Shao, Peiyi Wang, Qihao Zhu, Runxin Xu, Junxiao Song, Xiao Bi, Haowei Zhang, Mingchuan Zhang, YK Li, Y Wu, et al. Deepseekmath: Pushing the limits of mathematical reasoning in open language models. *arXiv preprint arXiv:2402.03300*, 2024.
- [35] Charlie Snell, Jaehoon Lee, Kelvin Xu, and Aviral Kumar. Scaling llm test-time compute optimally can be more effective than scaling model parameters. *arXiv preprint arXiv:2408.03314*, 2024.
- [36] Yi Su, Dian Yu, Linfeng Song, Juntao Li, Haitao Mi, Zhaopeng Tu, Min Zhang, and Dong Yu. Crossing the reward bridge: Expanding rl with verifiable rewards across diverse domains. *arXiv preprint arXiv:2503.23829*, 2025.
- [37] Fan-Yun Sun, Weiyu Liu, Siyi Gu, Dylan Lim, Goutam Bhat, Federico Tombari, Manling Li, Nick Haber, and Jiajun Wu. Layoutvlm: Differentiable optimization of 3d layout via vision-language models. *arXiv preprint arXiv:2412.02193*, 2024.
- [38] Jiapeng Tang, Yinyu Nie, Lev Markhasin, Angela Dai, Justus Thies, and Matthias Nießner. Diffuscene: Denoising diffusion models for generative indoor scene synthesis. In *Proceedings of the IEEE/CVF conference on computer vision and pattern recognition*, pages 20507–20518, 2024.
- [39] Yonglong Tian, Andrew Luo, Xingyuan Sun, Kevin Ellis, William T Freeman, Joshua B Tenenbaum, and Jiajun Wu. Learning to infer and execute 3d shape programs. *arXiv preprint arXiv:1901.02875*, 2019.
- [40] Kai Wang, Manolis Savva, Angel X Chang, and Daniel Ritchie. Deep convolutional priors for indoor scene synthesis. *ACM Transactions on Graphics (TOG)*, 37(4):1–14, 2018.
- [41] Xinpeng Wang, Chandan Yeshwanth, and Matthias Nießner. Sceneformer: Indoor scene generation with transformers. In *2021 International Conference on 3D Vision (3DV)*, pages 106–115. IEEE, 2021.
- [42] Xuezhi Wang, Jason Wei, Dale Schuurmans, Quoc Le, Ed Chi, Sharan Narang, Aakanksha Chowdhery, and Denny Zhou. Self-consistency improves chain of thought reasoning in language models. *arXiv preprint arXiv:2203.11171*, 2022.
- [43] Jason Wei, Maarten Bosma, Vincent Y Zhao, Kelvin Guu, Adams Wei Yu, Brian Lester, Nan Du, Andrew M Dai, and Quoc V Le. Finetuned language models are zero-shot learners. *arXiv preprint arXiv:2109.01652*, 2021.
- [44] Qiuhong Anna Wei, Sijie Ding, Jeong Joon Park, Rahul Sajjani, Adrien Poulenard, Srinath Sridhar, and Leonidas Guibas. Lego-net: Learning regular rearrangements of objects in rooms. In *Proceedings of the IEEE/CVF Conference on Computer Vision and Pattern Recognition*, pages 19037–19047, 2023.
- [45] Tomer Weiss, Alan Litteneker, Noah Duncan, Masaki Nakada, Chenfanfu Jiang, Lap-Fai Yu, and Demetri Terzopoulos. Fast and scalable position-based layout synthesis. *IEEE Transactions on Visualization and Computer Graphics*, 25(12):3231–3243, 2018.
- [46] Ken Xu, James Stewart, and Eugene Fiume. Constraint-based automatic placement for scene composition. In *Graphics Interface*, volume 2, pages 25–34. Citeseer, 2002.
- [47] An Yang, Baosong Yang, Beichen Zhang, Binyuan Hui, Bo Zheng, Bowen Yu, Chengyuan Li, Dayiheng Liu, Fei Huang, Haoran Wei, et al. Qwen2. 5 technical report. *arXiv preprint arXiv:2412.15115*, 2024.

- [48] Yixuan Yang, Junru Lu, Zixiang Zhao, Zhen Luo, James JQ Yu, Victor Sanchez, and Feng Zheng. Llplace: The 3d indoor scene layout generation and editing via large language model. *arXiv preprint arXiv:2406.03866*, 2024.
- [49] Yue Yang, Fan-Yun Sun, Luca Weihs, Eli VanderBilt, Alvaro Herrasti, Winson Han, Jiajun Wu, Nick Haber, Ranjay Krishna, Lingjie Liu, et al. Holodeck: Language guided generation of 3d embodied ai environments. In *Proceedings of the IEEE/CVF Conference on Computer Vision and Pattern Recognition*, pages 16227–16237, 2024.
- [50] Sifan Ye, Yixing Wang, Jiaman Li, Dennis Park, C Karen Liu, Huazhe Xu, and Jiajun Wu. Scene synthesis from human motion. In *SIGGRAPH Asia 2022 Conference Papers*, pages 1–9, 2022.
- [51] Hongwei Yi, Chun-Hao P Huang, Shashank Tripathi, Lea Hering, Justus Thies, and Michael J Black. Mime: Human-aware 3d scene generation. In *Proceedings of the IEEE/CVF Conference on Computer Vision and Pattern Recognition*, pages 12965–12976, 2023.
- [52] Lap Fai Yu, Sai Kit Yeung, Chi Keung Tang, Demetri Terzopoulos, Tony F Chan, and Stanley J Osher. Make it home: automatic optimization of furniture arrangement. *ACM Transactions on Graphics (TOG)-Proceedings of ACM SIGGRAPH 2011*, v. 30,(4), July 2011, article no. 86, 30 (4), 2011.
- [53] Guangyao Zhai, Evin Pinar Örnek, Shun-Cheng Wu, Yan Di, Federico Tombari, Nassir Navab, and Benjamin Busam. Commonsences: Generating commonsense 3d indoor scenes with scene graph diffusion. *Advances in Neural Information Processing Systems*, 36:30026–30038, 2023.
- [54] Guangyao Zhai, Evin Pinar Örnek, Dave Zhenyu Chen, Ruotong Liao, Yan Di, Nassir Navab, Federico Tombari, and Benjamin Busam. Echoscene: Indoor scene generation via information echo over scene graph diffusion. In *European Conference on Computer Vision*, pages 167–184. Springer, 2024.
- [55] Xiaohua Zhai, Basil Mustafa, Alexander Kolesnikov, and Lucas Beyer. Sigmoid loss for language image pre-training. In *Proceedings of the IEEE/CVF international conference on computer vision*, pages 11975–11986, 2023.
- [56] Yunzhi Zhang, Zizhang Li, Matt Zhou, Shangzhe Wu, and Jiajun Wu. The scene language: Representing scenes with programs, words, and embeddings. *arXiv preprint arXiv:2410.16770*, 2024.